

Research Article

Nascent SecM chain interacts with outer ribosomal surface to stabilize translation arrest

Mikihisa Muta¹,  Ryo Iizuka¹, Tatsuya Niwa², Yuanfang Guo¹, Hideki Taguchi² and Takashi Funatsu¹

¹Graduate School of Pharmaceutical Sciences, The University of Tokyo, 7-3-1 Hongo, Bunkyo-ku, Tokyo 113-0033, Japan; ²Cell Biology Center, Institute of Innovative Research, Tokyo Institute of Technology, 4259 Nagatsuta-cho, Midori-ku, Yokohama 226-8503, Japan

Correspondence: Ryo Iizuka (iizuka@mol.f.u-tokyo.ac.jp) or Takashi Funatsu (funatsu@mol.f.u-tokyo.ac.jp)



SecM, a bacterial secretion monitor protein, posttranscriptionally regulates downstream gene expression via translation elongation arrest. SecM contains a characteristic amino acid sequence called the arrest sequence at its C-terminus, and this sequence acts within the ribosomal exit tunnel to stop translation. It has been widely assumed that the arrest sequence within the ribosome tunnel is sufficient for translation arrest. We have previously shown that the nascent SecM chain outside the ribosomal exit tunnel stabilizes translation arrest, but the molecular mechanism is unknown. In this study, we found that residues 57–98 of the nascent SecM chain are responsible for stabilizing translation arrest. We performed alanine/serine-scanning mutagenesis of residues 57–98 to identify D79, Y80, W81, H84, R87, I90, R91, and F95 as the key residues responsible for stabilization. The residues were predicted to be located on and near an α -helix-forming segment. A striking feature of the α -helix is the presence of an arginine patch, which interacts with the negatively charged ribosomal surface. A photocross-linking experiment showed that Y80 is adjacent to the ribosomal protein L23, which is located next to the ribosomal exit tunnel when translation is arrested. Thus, the folded nascent SecM chain that emerges from the ribosome exit tunnel interacts with the outer surface of the ribosome to stabilize translation arrest.

Introduction

Translation is a fundamental biological process via which ribosomes decode genetic information in mRNA and convert it into amino acid sequences that form proteins. The process is strategically regulated to ensure that proteins are synthesized with precise timing and at specific subcellular locations in response to changes in the cellular environment [1,2]. Under some circumstances, translation arrest occurs at the elongation or termination step to control the expression of specific genes. This phenomenon, termed translation arrest, is genetically programmed and mediated by nascent (poly)peptides. Several such (poly)peptides have been identified in both prokaryotes and eukaryotes. They interact with the ribosome interior to block specific translation steps. Interestingly, they have little sequence similarity and induce translation arrest via distinct mechanisms; some require cofactors such as metabolites and antibiotics, whereas others do not [3,4]. The best characterized of these (poly)peptides is SecM from *Escherichia coli*.

E. coli SecM, a 170-amino-acid secretion protein, has a specific sequence at its C-terminus (150-FSTPVWISQAQGIRAGP-166) called the arrest sequence, which is required to induce translation elongation arrest [5,6]. SecM regulates the translation of the downstream gene *secA*, which encodes a secretion-driving ATPase, in response to protein secretion activity in the cell [7]. When a cell is secretion-proficient, nascent SecM is pulled by SecA in association with the SecYEG translocon immediately after translation arrest [8]. At this point, a secondary structure encompassing the *secA* Shine–Dalgarno sequence in the *secM*–*secA* mRNA inhibits *secA* translation [5,9]. However, under

Received: 27 September 2019
Revised: 6 January 2020
Accepted: 8 January 2020

Accepted Manuscript online:
8 January 2020
Version of Record published:
31 January 2020

secretion-defective conditions, SecM translation is subjected to prolonged arrest, inducing a conformational rearrangement in the mRNA that exposes the Shine–Dalgarno sequence. This in turn enables ribosome binding and subsequent *secA* translation [5–7,10].

The arrest sequence of SecM can cause translation arrest of unrelated proteins, which can be utilized to generate nascent chain–ribosome complexes (e.g. Ref. [11]). Hence, it is widely accepted that the SecM arrest sequence is necessary and sufficient for sustained translation arrest. However, recent investigations suggest that the arrest sequence alone is not always adequate to provide stable translation arrest when fused to the C-terminus of unrelated proteins [11–15]. For instance, we have demonstrated that the efficiency and stability of translation arrest correlates with the length of the spacer sequence between the HaloTag protein and the arrest sequence [14]. In addition, Goldman et al. [15] reported that nascent chain folding near the ribosome tunnel exit can result in translation arrest release via peptide stretching in the tunnel. The most likely explanation is that the SecM arrest sequence is susceptible to a pulling force exerted by the nascent chain outside the ribosome. Interestingly, we have found that the nascent SecM chain outside the ribosome exit tunnel helps stabilize the arrest [14]. However, the molecular mechanism underlying the stabilization is unknown. To clarify this issue, we performed mutational analysis of SecM and found that the folded nascent SecM chain interacts with the ribosomal surface to stabilize translation arrest.

Experimental

Prediction of the secondary structure

The secondary structure of *E. coli* SecM was predicted using the PSIPRED program (v3.3; <http://bioinf.cs.ucl.ac.uk/psipred/>) [16].

Preparation of templates for *in vitro* transcription and translation

To introduce the TC tag (CCPGCC) [17] into the N-terminus of SecM and SecM(Δ 1–37), the gene encoding SecM was amplified from pTA-SecM [14] using PCR with the primers shown in Supplementary Table S1. The PCR products were digested with *Nde* I and *Bam*H I and then ligated to the same sites in the pET23b vector (Merck Millipore) to yield the plasmids pTCSecM and pTCSecM(Δ 1–37). Deletion mutants of TC-SecM were generated from pTCSecM using the KOD -Plus- Mutagenesis Kit (Toyobo). Point mutations were introduced using the QuikChange Site-Directed Mutagenesis Kit (Agilent Technologies) or KOD -Plus- Mutagenesis Kit. An expression plasmid for HaloTag-SecM with a 23-amino acid glycine–serine linker [Halo-SecM(23GS)] was generated from pHaloSecM(8GS) [14] using the KOD -Plus- Mutagenesis Kit. The primer sets are presented in Supplementary Table S2–S4. The resultant plasmids were used as templates for PCR amplification to prepare template DNA for *in vitro* transcription and translation, as described previously [14,18].

Analyzing the translation arrest duration

Each construct was transcribed and translated using the PURE_{frex} 1.0 system (Gene Frontier Co., Ltd.) in a 20- μ l reaction containing 10 μ l of solution I, 1 μ l of solution II, 1 μ l of solution III, 2 μ l of template DNA, 1 μ l of SUPERase In RNase Inhibitor (Thermo Fisher Scientific), 1 μ l of 20 μ M FAsH-EDT₂ (Thermo Fisher Scientific), and 4 μ l of nuclease-free water (Qiagen). The mixtures were incubated for 20 min at 37°C, and then 2 mM puromycin (Sigma–Aldrich) was added to release nascent polypeptides from elongation-competent ribosomes and block elongation of newly initiated translation. After further incubation for the indicated time at 37°C, aliquots (4 μ l) were sampled and mixed with the same volume of the 2 \times sample buffer [125 mM Tris–HCl pH 6.8, 4% (w/v) SDS and 20% (v/v) glycerol] treated with RNasequre (Thermo Fisher Scientific) [19]. The sample buffer was employed to reduce background staining. SDS–PAGE was performed using NuPAGE 10% Bis-Tris Gel with MES SDS Running Buffer (Thermo Fisher Scientific) to detect polypeptidyl-tRNA [20]. Fluorescently-labeled polypeptides were visualized using the ChemiDoc Touch MP imaging system or Molecular Imager FX (Bio-Rad Laboratories). Band intensities were measured using ImageJ (<https://imagej.nih.gov/ij/>). Before image analysis, the background of each image was subtracted using the ImageJ rolling ball background subtraction algorithm. The lifetime of translation arrest for each construct was determined as described previously [14]. Data fitting was performed using the KaleidaGraph program (Synergy Software). Statistical analyses were performed using the R software (<https://www.r-project.org/>).

Photocross-linking assay

p-Benzoyl-L-phenylalanine (Bpa) [21] was introduced into TC-SecM and Halo-SecM(23GS) using the amber suppression method with the PURE_{flex} 1.0 system lacking release factor 1 (RF1) to avoid competition between the release factor and suppressor tRNA [22]. TC-SecM and TC-SecM(P166A) with an amber mutation at Y80, W81, or F95 were translated in the presence of an amber suppressor tRNA with Bpa (Bpa-tRNA; ProteinExpress Co., Ltd.). Each reaction contained 10 μ l of solution I, 1 μ l of solution II without RF1, 1 μ l of solution III, 2 μ l of template DNA, 2 μ l of Bpa-tRNA solution, and 4 μ l of nuclease-free water. The mixtures were incubated for 40 min at 37°C in the dark. After the addition of puromycin (2 mM), the mixtures were irradiated with a 355-nm laser (Genesis CX355-40 STM, Coherent) for 10 min at room temperature. The resultant products were stained with 2 μ M FLAsH-EDT₂ for 30 min at 37°C and then treated with 400 μ g/ml RNase A (Thermo Fisher Scientific) for 10 min at 37°C. Polypeptides were separated on 12% Laemmli SDS-PAGE gels. Fluorescently-labeled polypeptides were visualized using Molecular Imager FX. To identify a photocross-linking partner for SecM, Halo-SecM(23GS) with an amber mutation at Y80 was translated in a 120- μ l reaction for 60 min at 37°C and treated either with or without UV irradiation. The products were biotinylated using 1 μ M HaloTag PEG Biotin Ligand (Promega) and treated with RNase A. Unbound biotin ligands were removed using NAP5 columns (GE Healthcare). The biotinylated products were purified using streptavidin-modified magnetic beads (Dynabeads MyOne Streptavidin C1, Thermo Fisher Scientific), according to the manufacturer's instructions. Bound proteins were eluted by boiling in Laemmli sample buffer and then resolved on 7% Laemmli SDS-PAGE gels. Gels were stained with Coomassie Brilliant Blue (EzStain Aqua, ATTO corporation). Gel pieces of ~65 kDa were excised and digested in-gel with trypsin gold (Promega). The digested peptides were extracted with 50% acetonitrile. After evaporation using a centrifugal evaporator, the peptides were dissolved in 2% acetonitrile and 0.1% TFA solution and desalted with a C18 Stage Tip (Nikkyo Technos). The resulting peptides were subjected to liquid chromatography-tandem mass spectrometry (LC-MS/MS) as described elsewhere [23]. MS/MS spectra were searched against the GenoBase database [24] using the Sequest algorithm within Proteome Discoverer 2.1 (Thermo Fisher Scientific).

Results

Identification of the segment responsible for stable translation arrest

The nascent SecM chain outside the ribosome exit tunnel cannot be seen in the currently available cryoelectron microscopy structure [12,25,26]. We predicted the secondary structure of SecM using the PSIPRED program [16], which is one of the most popular and reliable methods available on the web. The prediction indicated that SecM forms several α -helices (Supplementary Figure S1). In considering the predicted structure and length of the ribosome exit tunnel (the tunnel can accommodate ~30 amino acids of a stretched peptide chain [27]), we constructed a series of deletion mutants of SecM [TC-SecM(Δ 1–37), TC-SecM(Δ 38–56), TC-SecM(Δ 57–73), TC-SecM(Δ 74–98), and TC-SecM(Δ 99–132)] to identify the segment responsible for stabilizing translation arrest. These mutants were fused with a tetracysteine (TC) tag at the N-terminus, enabling fluorescent labeling and translation product detection (Figure 1). The TC tag is composed of six amino acids CCPGCC, which covalently bind to biarsenical dyes such as FLAsH-EDT₂ with high affinity [17].

TC-SecM and the deletion mutants were translated in the presence of FLAsH-EDT₂ using a commercially available version of a reconstituted *E. coli* cell-free translation system (PURE system) [22] to examine the durations of translation arrest [14]. The products were treated with puromycin to release nascent polypeptides from elongation-competent ribosomes and block elongation of newly initiated translation. SecM-arrested ribosomes, which contain a prolyl-tRNA^{Pro} in the A site, prevent the entry of puromycin, but allow it when the arrest is released [20]. Then, aliquots of the mixture obtained at the indicated time points were separated using SDS-PAGE at a neutral pH to analyze the fraction of the translation arrest product (polypeptidyl-tRNA) remaining [14,20] (Supplementary Figure S2). The lifetime was determined by fitting a single exponential curve to the plot of the fraction against the incubation time with puromycin to evaluate the duration of translation arrest [14] (Supplementary Figure S2). The deletion of residues 1–37, corresponding to a secretion signal sequence [28], significantly prolonged the duration of translation arrest (Figure 1). Consistent with our result, the signal sequence has been shown to facilitate the release of translation arrest [10,29]. However, the absence of residues 57–73 and 74–98 significantly shortened the duration of translation arrest, whereas the absence of residues 38–56 and 99–132 did not (Figure 1). These results implied that residues within the region 57–98 are necessary for stable translation arrest.

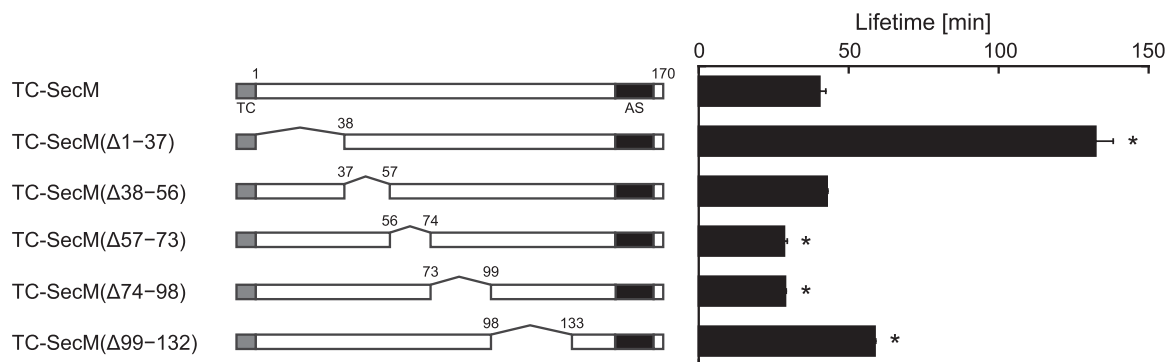


Figure 1. Lifetimes of translation arrest of deletion mutants.

(Left) Cartoon representations of TC-SecM and its segment deletion mutants. TC, TC tag; AS, arrest sequence. (Right) Lifetimes of TC-SecM and its deletion mutants. Values represent the mean \pm standard deviation of three independent experiments. Statistical significance was determined by Dunnett's multiple comparison of means testing (* $P < 0.001$). Representative gel images and quantitative data are shown in Supplementary Figure S2.

Identification of the residues responsible for stable translation arrest

Next, we performed alanine/serine-scanning mutagenesis of residues 57–98 to identify the amino acid residues important for stable translation arrest. A total of 42 TC-tagged mutants were translated in the PURE system, and the durations of translation arrest were examined (Supplementary Figure S3 and Figure 2A). Most of the mutants displayed shorter durations of translation arrest than the wild type. In particular, the durations of D79A, Y80A, W81A, H84A, R87A, I90A, R91A, and F95A mutants were <50% of that of the wild type (Figure 2A). The key residues responsible for stable translation arrest are expected to be present on and near helix 4, which is the predicted fourth α -helix composed of residues 81–95 (Supplementary Figure S1 and Figure 2B). Strikingly, H84, R87, and R91 will line one face of the helix, presuming the residues form a positively charged patch (Figure 2B). Substitutions of H84 for negatively and positively charged residues significantly reduced the duration of translation arrest (Supplementary Figure S4). However, substitutions of R87 and R91 for glutamate greatly diminished the durations of translation arrest, whereas substitutions for lysine did not (Supplementary Figure S5 and Figure 2C). These results indicate that positively charged residues at positions 87 and 91 are required for stable translation arrest. Given that the ribosome has a highly negatively charged surface [30], it is likely that the arginine residues associates directly with the ribosomal surface via electrostatic interactions, resulting in sustained translation arrest. On the other hand, mutation of Q83 to alanine significantly increased the duration of translation arrest (Figure 2A). Because Q83 is predicted to be located on helix 4 (Figure 2B) and alanine has the highest helix-forming propensity [31], the stability of translation arrest is assumed to be positively correlated with the structural stability of helix 4. Consistent with this idea, substitutions of Q83 for glycine and proline, which are normally unfavorable in α -helices [31], decreased the durations of translation arrest (Supplementary Figure S6). These findings support the hypothesis that the helical structure of a nascent SecM chain emerging from the ribosome exit tunnel is important in its potential interaction with the ribosomal surface.

Photocross-linking between SecM and the ribosome

To demonstrate spatial proximity between helix 4 of SecM and the ribosomal surface, we employed a site-specific photocross-linking approach using the photoreactive amino acid Bpa. Bpa generates biradical species upon irradiation with UV light (350–365 nm), and the species react covalently with carbon-hydrogen bonds within 3 Å [21]. Aromatic residues (Y80, W81, and F95) were selected to be substituted with Bpa, because the aromatic character of Bpa substantially affected the stability of translation arrest such as in the case of R87 (Supplementary Figure S7). The translation products of Y80Bpa, W81Bpa, and F95Bpa mutants were subjected to UV irradiation and separated using SDS-PAGE with RNase A pretreatment. TC-SecM, not containing Bpa, predominantly migrated as a band of ~20 kDa (Figure 3, lane 1), whereas the Y80Bpa, W81Bpa, and F95Bpa mutants rendered multiple bands (Figure 3, lanes 2, 5, and 8), indicating that the bands with apparently higher

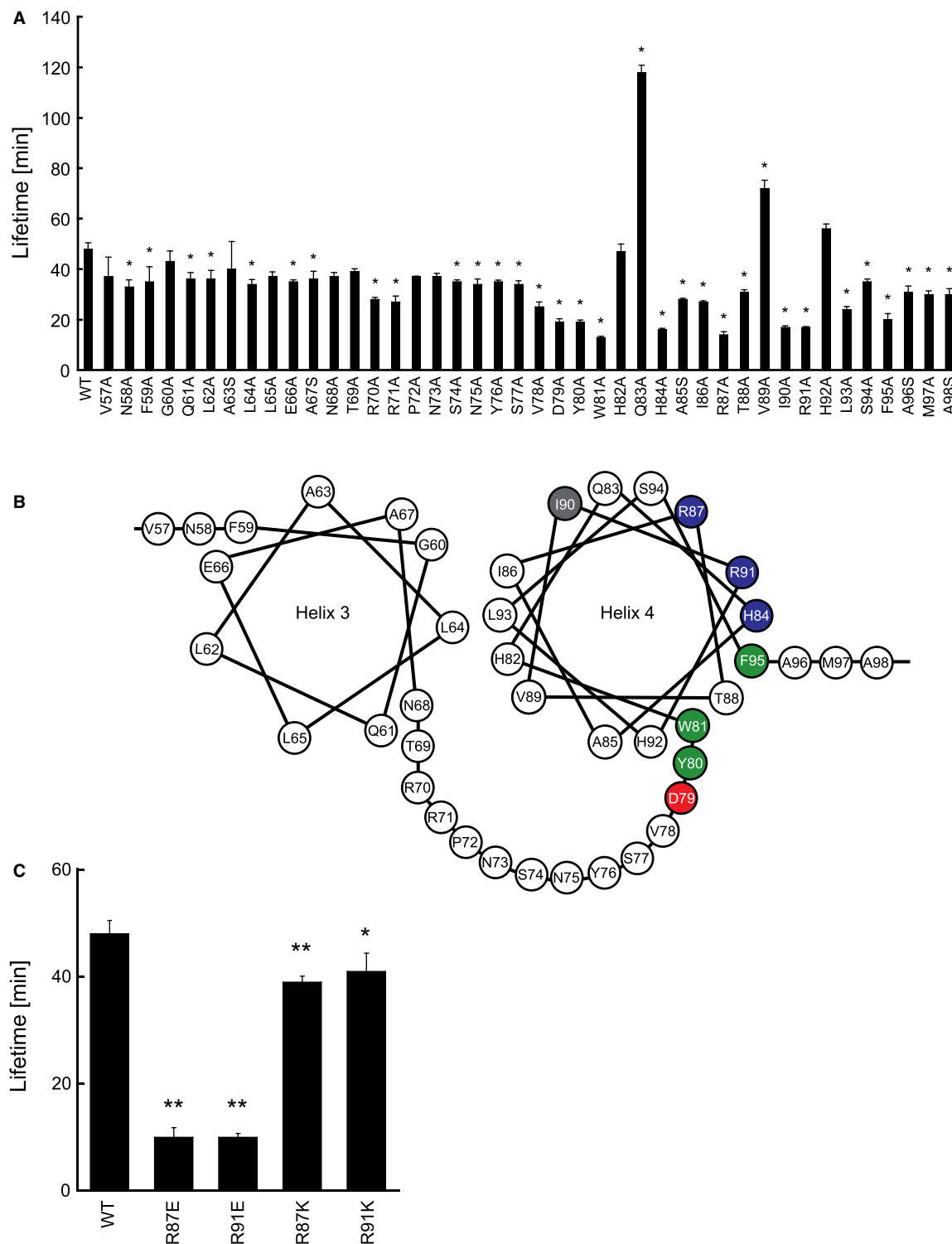


Figure 2. Lifetimes of translation arrest of alanine/serine-scanning mutants.

Part 1 of 2

(A) Lifetimes of translation arrest for TC-SecM (WT) and alanine/serine-scanning mutants. Values represent the mean \pm standard deviation of three or four independent experiments. Statistical significance was determined by Dunnett's multiple comparison of means testing ($* P < 0.001$). Representative gel images and quantitative data are shown in Supplementary Figure S3. (B) Predicted structure of residues 57–98. The structure was predicted by PSIPRED v3.3 (Supplementary Figure S1). The highlighted amino acid residues are critical to stable translation arrest: positively and negatively charged, and aromatic

Figure 2. Lifetimes of translation arrest of alanine/serine-scanning mutants.

Part 2 of 2

residues are colored blue, red, and green, respectively. (C) Effect of positive charge at residues 87 and 91 on the lifetime of translation arrest. Values represent the mean \pm standard deviation of three or four independent experiments. The value for the WT was taken from Figure 2A. Statistical significance was determined by Dunnett's multiple comparison of means testing (* $P < 0.01$, ** $P < 0.001$). Representative gel images and quantitative data are shown in Supplementary Figure S5.

molecular masses correspond to photocross-linked products. RNase A treatment did not alter the mobility of the products (Supplementary Figure S8), suggesting that SecM was linked to proteins. Intriguingly, the introduction of the arrest-weakened mutation (R87A) (Figure 2A) into the mutants reduced the apparent 32-kDa-photocross-linked products (Figure 3, lanes 3, 6, and 9). Also, the introduction of the arrest-deficient mutation (P166A) [6] completely eliminated the products (Figure 3, lanes 4, 7, and 10). These results indicate that the cross-linking degree is compatible with the stability of translation arrest.

The notable cross-linking product of SecM(Y80Bpa) was analyzed using mass spectrometry to identify the cross-linking partner, because the translation arrest stability of TC-SecM(Y80Bpa) was similar to that of TC-SecM (Supplementary Figure S7). SecM(Y80Bpa) was translated in fusion with the C-terminus of HaloTag via a 23-amino acid GS linker, which enabled purification of the cross-linking product through a biotin-strep-avidin interaction [32]. We have previously shown that the fusion of HaloTag to SecM does not affect the stability of translation arrest [14]. The translation products of Halo-SecM(Y80Bpa) with and without UV irradiation were purified and resolved using SDS-PAGE. UV irradiation resulted in a cross-linking product with a molecular mass of 65 kDa, whereas no cross-linking product was observed without UV irradiation (Supplementary Figure S9). In the absence and presence of UV irradiation, gel pieces containing 65 kDa proteins were excised, treated with trypsin, and subjected to analysis by LC-MS/MS. Two independently prepared samples were analyzed. To reduce false positive identifications, a cutoff was applied where proteins had at least two peptide annotations per protein (number of peptides ≥ 2) under UV irradiation. All of those proteins are listed in Supplementary Table S5. A total of 27 proteins were found in two samples, of which 9 met the

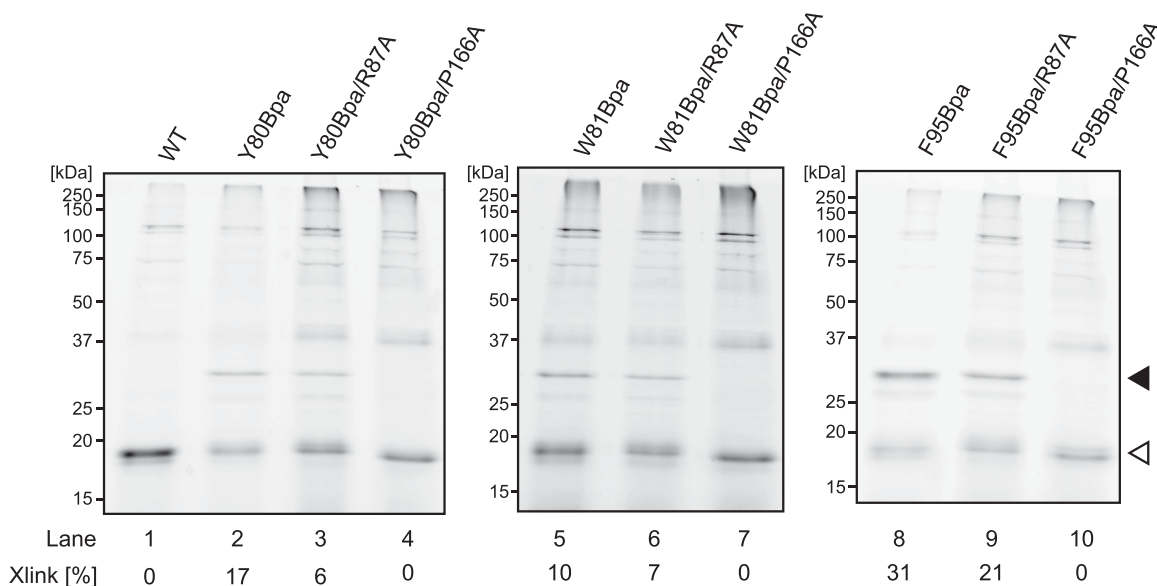


Figure 3. Detection of photocross-linked protein with TC-SecM.

TC-SecM, TC-SecM(R87A), and TC-SecM(P166A) with an amber mutation at Y80, W81, or F95 were translated in the presence of amber suppressor tRNA with Bpa. The products were exposed to UV irradiation and treated with RNase A. Polypeptides labeled with FIAsh were separated by SDS-PAGE. Black and white arrowheads indicate the apparent 32 kDa-cross-linked and released products, respectively. Xlink indicates the percentage of the intensity of the band indicated by black arrowhead in each lane. The results shown are representative of three independent experiments with similar results.

requirement (<20 kDa) for the cross-linking partner of SecM (Table 1). Among them, the ribosomal protein L23, which is located next to the ribosomal exit tunnel on the 50S ribosomal subunit [33,34], showed a significant increase in the number of peptide spectrum matches after being exposed to UV light (Table 1). The result suggests that helix 4 of SecM is in close proximity to L23, due to a specific interaction between SecM and the outer surface of the ribosome.

Discussion

In this study, we examined the molecular mechanism via which the nascent SecM chain outside the ribosomal exit tunnel stabilizes translation arrest. First, we showed that the residues 57–98 are important for stable translation arrest (Figure 1), which is consistent with the findings of an earlier study [35]. Second, we found that the stability of SecM translation arrest can be modulated by single amino acid changes in the residues 57–98 (Figure 2 and Supplementary Figures S4, S5). Alanine/serine-scanning mutagenesis identified eight key residues (D79, Y80, W81, H84, R87, I90, R91, and F95) responsible for stabilization (Figure 2A). These residues were predicted to be located near and on helix 4 of SecM (Figures 1, 2B). Positively charged residues at position 87 and 91 were shown to be essential for stable translation arrest, suggesting that the residues may interact with the negatively charged ribosome surface (Figure 2C). Finally, we demonstrated the spatial proximity of the helix and ribosome surface. A photocross-linking experiment showed that when translation is arrested, Y80 is located adjacent to ribosomal protein L23, which is near the nascent chain exit site of the ribosome (Figure 3 and Table 1). L23 is a universal ribosomal protein, which serves as the docking site for nascent chain-associated factors that facilitate protein folding, maturation, and localization, including trigger factor [36,37], methionine

Table 1 LC-MS/MS identification of proteins contained in the photocross-linking product

Protein	Accession Number	Mw (kDa)	Replicate 1					Replicate 2				
			Number of peptides		Number of peptide spectrum matches			Number of peptides		Number of peptide spectrum matches		
			+UV	–UV	+UV	–UV	ΔPSMs	+UV	–UV	+UV	–UV	ΔPSMs
Halo-SecM (Y80Bpa)		53.913	10	9	111	53	58	10	11	116	65	51
50S ribosomal protein L23	JW3280	11.192	5		45		45	4		35		35
50S ribosomal protein L17	JW3256	14.356	2	1	6	3	3	3	3	11	8	3
30S ribosomal protein S11	JW3259	13.836	3	2	9	6	3	3	3	9	9	0
30S ribosomal protein S13	JW3260	13.091	3	3	8	7	1	4	4	11	12	–1
50S ribosomal protein L14	JW3272	13.532	3	2	7	6	1	2	2	6	6	0
50S ribosomal protein L20	JW1706	13.489	4	4	11	12	–1	4	4	9	10	–1
50S ribosomal protein L28	JW3612	9.001	2	2	5	6	–1	3	1	8	2	6
50S ribosomal protein L6	JW3267	18.892	2	4	6	10	–4	2		4		4
30S ribosomal protein S21	JW3037	8.495	2	4	5	14	–9	4	3	13	12	1

Proteins with a molecular mass of <20 kDa are adapted from Supplementary Table S5. The number of peptides and peptide spectrum matches (PSMs) represent the total number of distinct peptide sequences identified in the protein and the total number of identified peptide sequences (peptide spectrum matches), respectively. +UV, with UV irradiation; –UV, without UV irradiation; ΔPSMs, (the number of PSMs)_{+UV}–(the number of PSMs)_{–UV}.

aminopeptidase [38], signal recognition particle [39–41], SecA [42,43], SecYEG [44,45], and YidC [46]. Interestingly, the bacterial L23 protein has an exposed negatively charged patch on its surface [47], which implies that the patch interacts with R87 and R91 of SecM. The neighboring residues such as D79, Y80, W81, H84, and F95 appear to contribute to the interaction with L23 protein. The distal residue I90 could play an important role in providing a supportive environment for the interaction (Figure 2B).

Taken together, we propose the following mechanism via which the nascent SecM chain outside the ribosomal exit tunnel stabilizes translation arrest. When the arrest sequence of SecM is translated and properly placed in the exit tunnel, it induces a conformational change in the ribosome, inhibiting the peptidyltransferase reaction [6,20,48]. At this point, the nascent chain that is emerging from the ribosome exit tunnel folds or has folded to form α -helices. Then, the region containing helix 4 docks onto the L23 protein, resulting in sustained translation arrest. The SecM arrest sequence is shown to be susceptible to a pulling force acting on the nascent chain [13–15,49–51]. For example, translation arrest is prevented by the cotranslational folding of HaloTag [32] and Top7 (an artificial 93-residue protein) [52] just outside the exit tunnel, which can exert a pulling force on the nascent chain [14,15]. The arrest sequence has been employed as a probe to detect folding events inside and outside the ribosomal tunnel [53–60]. Therefore, the interaction between SecM and the outer surface of the ribosome is considered to contribute to the formation of a long-lived arrested complex, inhibition of translation elongation, and induction of downstream *secA* expression.

In *E. coli*, translation arrest is released promptly under physiologically appropriate conditions [5,10]; the interaction of SecM with the outer surface of the ribosome is easily disrupted during the Sec-mediated export process. As mentioned above, SecA is shown to bind to ribosome through an interaction with the L23 protein [42,43], which suggests that SecA and SecM compete to bind with the L23 protein. Hence, when sufficiently available, SecA is likely to competitively interfere with the interaction of SecM with the L23 protein and release the translation arrest by mechanically pulling SecM in association with the SecYEG translocon [8]. To explain the mechanism Furthermore, we will need to study the molecular interplay between the ribosome, SecM, SecA, and SecYEG during protein sorting and translocation.

SecM protein sequences are considered optimal to render stable translation arrest, because the key residues that enable this stability are strictly conserved among SecM orthologs from *Enterobacteriales* (Supplementary Figure S10). Secondary structure predictions show that the position of these residues is conserved; they are predicted to be near and on an α -helix, which corresponds to helix 4 of SecM from *E. coli* (Supplementary Figures S10, S11). The substitution of residues 57–73 did not markedly alter the duration of translation arrest (Figure 2A). As the deletion of residues 57–73 significantly reduces the stability of translation arrest (Figure 1), the region is likely to support the folding of helix 4 and/or the interaction with nascent SecM chain and the ribosome. The connectivity of residues and secondary structure elements could be a key determinant of stable translation arrest. Although SecM exhibits limited phylogenetic distribution [61], it can be argued that SecM is a highly sophisticated regulatory protein.

Abbreviations

Bpa, *p*-benzoyl-L-phenylalanine; LC–MS/MS, liquid chromatography–tandem mass spectrometry; PSMs, number of peptides and peptide spectrum matches; RF1, release factor 1; TC, tetracysteine.

Author Contribution

R.I. and T.F. conceived the study and designed the experiments; M.M., R.I. and Y.G. performed the experiments and analyzed the data; T.N. and H.T. performed the LC–MS/MS analysis; and M.M., R.I. and T.F. wrote the manuscript.

Funding

This study was supported by JSPS KAKENHI Grant Numbers 26116002, JP15H01527, JP17H05660, JP17K15073, JP18H03981, JP18H03984, JP18K05330, and JST COI Grant Number JPMJCE1305. This study was also supported by JST Research Complex Program and JSPS Core-to-Core Program, A. Advanced Research Networks.

Open Access

Open access for this article was enabled by the participation of The University of Tokyo in an all-inclusive *Read & Publish* pilot with Portland Press and the Biochemical Society.

Competing Interests

The authors declare that there are no competing interests associated with the manuscript.

References

- 1 Brar, G.A. and Weissman, J.S. (2015) Ribosome profiling reveals the what, when, where and how of protein synthesis. *Nat. Rev. Mol. Cell Biol.* **16**, 651–664 <https://doi.org/10.1038/nrm4069>
- 2 Stein, K.C. and Frydman, J. (2019) The stop-and-go traffic regulating protein biogenesis: how translation kinetics controls proteostasis. *J. Biol. Chem.* **294**, 2076–2084 <https://doi.org/10.1074/jbc.REV118.002814>
- 3 Ito, K. and Chiba, S. (2013) Arrest peptides: *cis*-acting modulators of translation. *Annu. Rev. Biochem.* **82**, 171–202 <https://doi.org/10.1146/annurev-biochem-080211-105026>
- 4 Wilson, D.N., Arenz, S. and Beckmann, R. (2016) Translation regulation via nascent polypeptide-mediated ribosome stalling. *Curr. Opin. Struct. Biol.* **37**, 123–133 <https://doi.org/10.1016/j.sbi.2016.01.008>
- 5 Nakatogawa, H. and Ito, K. (2001) Secretion monitor, SecM, undergoes self-translation arrest in the cytosol. *Mol. Cell* **7**, 185–192 [https://doi.org/10.1016/S1097-2765\(01\)00166-6](https://doi.org/10.1016/S1097-2765(01)00166-6)
- 6 Nakatogawa, H. and Ito, K. (2002) The ribosomal exit tunnel functions as a discriminating gate. *Cell* **108**, 629–636 [https://doi.org/10.1016/S0092-8674\(02\)00649-9](https://doi.org/10.1016/S0092-8674(02)00649-9)
- 7 Oliver, D., Norman, J. and Sarker, S. (1998) Regulation of *Escherichia coli* *secA* by cellular protein secretion proficiency requires an intact gene X signal sequence and an active translocon. *J. Bacteriol.* **180**, 5240–5242 <https://doi.org/10.1128/JB.180.19.5240-5242.1998>
- 8 Butkus, M.E., Prundeanu, L.B. and Oliver, D.B. (2003) Translocon “pulling” of nascent SecM controls the duration of its translational pause and secretion-responsive *secA* regulation. *J. Bacteriol.* **185**, 6719–6722 <https://doi.org/10.1128/JB.185.22.6719-6722.2003>
- 9 McNicholas, P., Salavati, R. and Oliver, D. (1997) Dual regulation of *Escherichia coli* *secA* translation by distinct upstream elements. *J. Mol. Biol.* **265**, 128–141 <https://doi.org/10.1006/jmbi.1996.0723>
- 10 Sarker, S. and Oliver, D. (2002) Critical regions of *secM* that control its translation and secretion and promote secretion-specific *secA* regulation. *J. Bacteriol.* **184**, 2360–2369 <https://doi.org/10.1128/JB.184.9.2360-2369.2002>
- 11 Evans, M.S., Ugrinov, K.G., Frese, M.A. and Clark, P.L. (2005) Homogeneous stalled ribosome nascent chain complexes produced *in vivo* or *in vitro*. *Nat. Methods* **2**, 757–762 <https://doi.org/10.1038/nmeth790>
- 12 Bhushan, S., Hoffmann, T., Seidelt, B., Frauenfeld, J., Mielke, T., Berninghausen, O. et al. (2011) SecM-stalled ribosomes adopt an altered geometry at the peptidyl transferase center. *PLoS Biol.* **9**, e1000581 <https://doi.org/10.1371/journal.pbio.1000581>
- 13 Ismail, N., Hedman, R., Schiller, N. and von Heijne, G. (2012) A biphasic pulling force acts on transmembrane helices during translocon-mediated membrane integration. *Nat. Struct. Mol. Biol.* **19**, 1018–1022 <https://doi.org/10.1038/nsmb.2376>
- 14 Yang, Z., Iizuka, R. and Funatsu, T. (2015) Nascent SecM chain outside the ribosome reinforces translation arrest. *PLoS ONE* **10**, e0122017 <https://doi.org/10.1371/journal.pone.0122017>
- 15 Goldman, D.H., Kaiser, C.M., Milin, A., Righini, M., Tinoco, Jr, I. and Bustamante, C. (2015) Mechanical force releases nascent chain-mediated ribosome arrest *in vitro* and *in vivo*. *Science* **348**, 457–460 <https://doi.org/10.1126/science.1261909>
- 16 McGuffin, L.J., Bryson, K. and Jones, D.T. (2000) The PSIPRED protein structure prediction server. *Bioinformatics* **16**, 404–405 <https://doi.org/10.1093/bioinformatics/16.4.404>
- 17 Adams, S.R., Campbell, R.E., Gross, L.A., Martin, B.R., Walkup, G.K., Yao, Y. et al. (2002) New biarsenical ligands and tetracysteine motifs for protein labeling *in vitro* and *in vivo*: synthesis and biological applications. *J. Am. Chem. Soc.* **124**, 6063–6076 <https://doi.org/10.1021/ja017687n>
- 18 Iizuka, R., Yamagishi-Shirasaki, M. and Funatsu, T. (2011) Kinetic study of *de novo* chromophore maturation of fluorescent proteins. *Anal. Biochem.* **414**, 173–178 <https://doi.org/10.1016/j.ab.2011.03.036>
- 19 Ito, K., Chadani, Y., Nakamori, K., Chiba, S., Akiyama, Y. and Abo, T. (2011) Nascentome analysis uncovers futile protein synthesis in *Escherichia coli*. *PLoS ONE* **6**, e28413 <https://doi.org/10.1371/journal.pone.0028413>
- 20 Muto, H., Nakatogawa, H. and Ito, K. (2006) Genetically encoded but nonpolypeptide prolyl-tRNA functions in the A site for SecM-mediated ribosomal stall. *Mol. Cell* **22**, 545–552 <https://doi.org/10.1016/j.molcel.2006.03.033>
- 21 Dormán, G. and Prestwich, G.D. (1994) Benzophenone photophores in biochemistry. *Biochemistry* **33**, 5661–5673 <https://doi.org/10.1021/bi00185a001>
- 22 Shimizu, Y., Inoue, A., Tomari, Y., Suzuki, T., Yokogawa, T., Nishikawa, K. et al. (2001) Cell-free translation reconstituted with purified components. *Nat. Biotechnol.* **19**, 751–755 <https://doi.org/10.1038/90802>
- 23 Sugita, S., Watanabe, K., Hashimoto, K., Niwa, T., Uemura, E., Taguchi, H. et al. (2018) Electrostatic interactions between middle domain motif-1 and the AAA1 module of the bacterial ClpB chaperone are essential for protein disaggregation. *J. Biol. Chem.* **293**, 19228–19239 <https://doi.org/10.1074/jbc.RA118.005496>
- 24 Otsuka, Y., Muto, A., Takeuchi, R., Okada, C., Ishikawa, M., Nakamura, K. et al. (2015) Genobase: comprehensive resource database of *Escherichia coli* K-12. *Nucleic Acids Res.* **43**, D606–D617 <https://doi.org/10.1093/nar/gku1164>
- 25 Mitra, K., Schaffitzel, C., Fabiola, F., Chapman, M.S., Ban, N. and Frank, J. (2006) Elongation arrest by SecM via a cascade of ribosomal RNA rearrangements. *Mol. Cell* **22**, 533–543 <https://doi.org/10.1016/j.molcel.2006.05.003>
- 26 Zhang, J., Pan, X., Yan, K., Sun, S., Gao, N. and Sui, S.F. (2015) Mechanisms of ribosome stalling by SecM at multiple elongation steps. *eLife* **4**, e09684 <https://doi.org/10.7554/eLife.09684>
- 27 Voss, N.R., Gerstein, M., Steitz, T.A. and Moore, P.B. (2006) The geometry of the ribosomal polypeptide exit tunnel. *J. Mol. Biol.* **360**, 893–906 <https://doi.org/10.1016/j.jmb.2006.05.023>
- 28 Sarker, S., Rudd, K.E. and Oliver, D. (2000) Revised translation start site for *secM* defines an atypical signal peptide that regulates *Escherichia coli* *secA* expression. *J. Bacteriol.* **182**, 5592–5595 <https://doi.org/10.1128/JB.182.19.5592-5595.2000>
- 29 Yap, M.N. and Bernstein, H.D. (2011) The translational regulatory function of SecM requires the precise timing of membrane targeting. *Mol. Microbiol.* **81**, 540–553 <https://doi.org/10.1111/j.1365-2958.2011.07713.x>

- 30 Knight, A.M., Culviner, P.H., Kurt-Yilmaz, N., Zou, T., Ozkan, S.B. and Cavagnero, S. (2013) Electrostatic effect of the ribosomal surface on nascent polypeptide dynamics. *ACS Chem. Biol.* **8**, 1195–1204 <https://doi.org/10.1021/cb400030n>
- 31 Pace, C.N. and Scholtz, J.M. (1998) A helix propensity scale based on experimental studies of peptides and proteins. *Biophys. J.* **75**, 422–427 [https://doi.org/10.1016/S0006-3495\(98\)77529-0](https://doi.org/10.1016/S0006-3495(98)77529-0)
- 32 Los, G.V., Encell, L.P., McDougall, M.G., Hartzell, D.D., Karassina, N., Zimprich, C. et al. (2008) Halotag: a novel protein labeling technology for cell imaging and protein analysis. *ACS Chem. Biol.* **3**, 373–382 <https://doi.org/10.1021/cb800025k>
- 33 Ban, N., Nissen, P., Hansen, J., Moore, P.B. and Steitz, T.A. (2000) The complete atomic structure of the large ribosomal subunit at 2.4 Å resolution. *Science* **289**, 905–920 <https://doi.org/10.1126/science.289.5481.905>
- 34 Harms, J., Schluenzen, F., Zarivach, R., Bashan, A., Gat, S., Agmon, I. et al. (2001) High resolution structure of the large ribosomal subunit from a mesophilic eubacterium. *Cell* **107**, 679–688 [https://doi.org/10.1016/S0092-8674\(01\)00546-3](https://doi.org/10.1016/S0092-8674(01)00546-3)
- 35 Nakamori, K., Chiba, S. and Ito, K. (2014) Identification of a SecM segment required for export-coupled release from elongation arrest. *FEBS Lett.* **588**, 3098–3103 <https://doi.org/10.1016/j.febslet.2014.06.038>
- 36 Kramer, G., Rauch, T., Rist, W., Vorderwulbecke, S., Patzelt, H., Schulze-Specking, A. et al. (2002) L23 protein functions as a chaperone docking site on the ribosome. *Nature* **419**, 171–174 <https://doi.org/10.1038/nature01047>
- 37 Schlünzen, F., Wilson, D.N., Tian, P., Harms, J.M., McInnes, S.J., Hansen, H.A. et al. (2005) The binding mode of the trigger factor on the ribosome: implications for protein folding and SRP interaction. *Structure* **13**, 1685–1694 <https://doi.org/10.1016/j.str.2005.08.007>
- 38 Sandikci, A., Gloge, F., Martinez, M., Mayer, M.P., Wade, R., Bukau, B. et al. (2013) Dynamic enzyme docking to the ribosome coordinates N-terminal processing with polypeptide folding. *Nat. Struct. Mol. Biol.* **20**, 843–850 <https://doi.org/10.1038/nsmb.2615>
- 39 Pool, M.R., Stumm, J., Fulga, T.A., Sinning, I. and Dobberstein, B. (2002) Distinct modes of signal recognition particle interaction with the ribosome. *Science* **297**, 1345–1348 <https://doi.org/10.1126/science.1072366>
- 40 Gu, S.Q., Peske, F., Wieden, H.J., Rodnina, M.V. and Wintermeyer, W. (2003) The signal recognition particle binds to protein L23 at the peptide exit of the *Escherichia coli* ribosome. *RNA* **9**, 566–573 <https://doi.org/10.1261/rna.2196403>
- 41 Schaffitzel, C., Oswald, M., Berger, I., Ishikawa, T., Abrahams, J.P., Koerten, H.K. et al. (2006) Structure of the *E. coli* signal recognition particle bound to a translating ribosome. *Nature* **444**, 503–506 <https://doi.org/10.1038/nature05182>
- 42 Huber, D., Rajagopalan, N., Preissler, S., Rocco, M.A., Merz, F., Kramer, G. et al. (2011) SecA interacts with ribosomes in order to facilitate posttranslational translocation in bacteria. *Mol. Cell* **41**, 343–353 <https://doi.org/10.1016/j.molcel.2010.12.028>
- 43 Singh, R., Kraft, C., Jaiswal, R., Sejwal, K., Kasaragod, V.B., Kuper, J. et al. (2014) Cryo-electron microscopic structure of SecA protein bound to the 70S ribosome. *J. Biol. Chem.* **289**, 7190–7199 <https://doi.org/10.1074/jbc.M113.506634>
- 44 Mitra, K., Schaffitzel, C., Shaikh, T., Tama, F., Jenni, S., Brooks, C.L.I.I. et al. (2005) Structure of the *E. coli* protein-conducting channel bound to a translating ribosome. *Nature* **438**, 318–324 <https://doi.org/10.1038/nature04133>
- 45 Frauenfeld, J., Gumbart, J., Sluis, E.O., Funes, S., Gartmann, M., Beatrix, B. et al. (2011) Cryo-EM structure of the ribosome-SecYE complex in the membrane environment. *Nat. Struct. Mol. Biol.* **18**, 614–621 <https://doi.org/10.1038/nsmb.2026>
- 46 Kedrov, A., Wickles, S., Crevenna, A.H., van der Sluis, E.O., Buschauer, R., Berninghausen, O. et al. (2016) Structural dynamics of the YidC:Ribosome complex during membrane protein biogenesis. *Cell Rep.* **17**, 2943–2954 <https://doi.org/10.1016/j.celrep.2016.11.059>
- 47 Öhman, A., Rak, A., Dontsova, M., Garber, M.B. and Härd, T. (2003) NMR structure of the ribosomal protein L23 from *Thermus thermophilus*. *J. Biomol. NMR* **26**, 131–137 <https://doi.org/10.1023/A:1023502307069>
- 48 Woolhead, C.A., Johnson, A.E. and Bernstein, H.D. (2006) Translation arrest requires two-way communication between a nascent polypeptide and the ribosome. *Mol. Cell* **22**, 587–598 <https://doi.org/10.1016/j.molcel.2006.05.021>
- 49 Cymer, F. and von Heijne, G. (2013) Cotranslational folding of membrane proteins probed by arrest-peptide-mediated force measurements. *Proc. Natl Acad. Sci. U.S.A.* **110**, 14640–14645 <https://doi.org/10.1073/pnas.1306787110>
- 50 Cymer, F., Ismail, N. and von Heijne, G. (2014) Weak pulling forces exerted on N_{in}-orientated transmembrane segments during co-translational insertion into the inner membrane of *Escherichia coli*. *FEBS Lett.* **588**, 1930–1934 <https://doi.org/10.1016/j.febslet.2014.03.050>
- 51 Ismail, N., Hedman, R., Lindén, M. and von Heijne, G. (2015) Charge-driven dynamics of nascent-chain movement through the SecYEG translocon. *Nat. Struct. Mol. Biol.* **22**, 145–149 <https://doi.org/10.1038/nsmb.2940>
- 52 Kuhlman, B., Dantas, G., Ireton, G.C., Varani, G., Stoddard, B.L. and Baker, D. (2003) Design of a novel globular protein fold with atomic-level accuracy. *Science* **302**, 1364–1368 <https://doi.org/10.1126/science.1089427>
- 53 Nilsson, O.B., Hedman, R., Marino, J., Wickles, S., Bischoff, L., Johansson, M. et al. (2015) Cotranslational protein folding inside the ribosome exit tunnel. *Cell Rep.* **12**, 1533–1540 <https://doi.org/10.1016/j.celrep.2015.07.065>
- 54 Nilsson, O.B., Nickson, A.A., Hollins, J.J., Wickles, S., Steward, A., Beckmann, R. et al. (2017) Cotranslational folding of spectrin domains via partially structured states. *Nat. Struct. Mol. Biol.* **24**, 221–225 <https://doi.org/10.1038/nsmb.3355>
- 55 Fariás-Rico, J.A., Goetz, S.K., Marino, J. and von Heijne, G. (2017) Mutational analysis of protein folding inside the ribosome exit tunnel. *FEBS Lett.* **591**, 155–163 <https://doi.org/10.1002/1873-3468.12504>
- 56 Fariás-Rico, J.A., Ruud Selin, F., Myronidi, I., Frühauf, M. and von Heijne, G. (2018) Effects of protein size, thermodynamic stability, and net charge on cotranslational folding on the ribosome. *Proc. Natl Acad. Sci. U.S.A.* **115**, E9280–E9287 <https://doi.org/10.1073/pnas.1812756115>
- 57 Tian, P., Steward, A., Kudva, R., Su, T., Shilling, P.J., Nickson, A.A. et al. (2018) Folding pathway of an Ig domain is conserved on and off the ribosome. *Proc. Natl Acad. Sci. U.S.A.* **115**, E11284–E11293 <https://doi.org/10.1073/pnas.1810523115>
- 58 Marsden, A.P., Hollins, J.J., O'Neill, C., Ryzhov, P., Higson, S., Mendonça, C.A.T.F. et al. (2018) Investigating the effect of chain connectivity on the folding of a beta-sheet protein on and off the ribosome. *J. Mol. Biol.* **430**, 5207–5216 <https://doi.org/10.1016/j.jmb.2018.10.011>
- 59 Kudva, R., Tian, P., Pardo-Avila, F., Carroni, M., Best, R.B., Bernstein, H.D. et al. (2018) The shape of the bacterial ribosome exit tunnel affects cotranslational protein folding. *eLife* **7**, e36326 <https://doi.org/10.7554/eLife.36326>
- 60 Notari, L., Martínez-Carranza, M., Fariás-Rico, J.A., Stenmark, P. and von Heijne, G. (2018) Cotranslational folding of a pentarepeat β-helix protein. *J. Mol. Biol.* **430**, 5196–5206 <https://doi.org/10.1016/j.jmb.2018.10.016>
- 61 van der Sluis, E.O. and Driessen, A.J. (2006) Stepwise evolution of the Sec machinery in Proteobacteria. *Trends Microbiol.* **14**, 105–108 <https://doi.org/10.1016/j.tim.2006.01.009>